

Effect of *Hypericum perforatum L.* Extract on Insulin Resistance and Lipid Metabolic Disorder in High-Fat-Diet Induced Obese Mice

Jin-ying Tian,¹ Rong-ya Tao,¹ Xiao-lin Zhang,¹ Qian Liu,¹ Yi-bo He,¹ Ya-lun Su,² Teng-fei Ji^{2*} and Fei Ye^{1*}

¹Beijing Key Laboratory of New Drug Mechanisms and Pharmacological Evaluation Study, Institute of Materia Medica, Chinese Academy of Medical Sciences, Beijing 100050, China

²State Key Laboratory of Bioactive Substance and Function of Natural Medicines, Institute of Materia Medica, Chinese Academy of Medical Sciences, Beijing 100050, China

Natural product *Hypericum perforatum L.* has been used in folk medicine to improve mental performance. However, the effect of *H. perforatum L.* on metabolism is still unknown. In order to test whether *H. perforatum L.* extract (EHP) has an effect on metabolic syndrome, we treated diet induced obese (DIO) C57BL/6J mice with the extract. The chemical characters of EHP were investigated with thin-layer chromatography, ultraviolet, high-performance liquid chromatography (HPLC), and HPLC-mass spectrometry fingerprint analysis. Oral glucose tolerance test (OGTT), insulin tolerance test (ITT), and the glucose infusion rate (GIR) in hyperinsulinemic–euglycemic clamp test were performed to evaluate the glucose metabolism and insulin sensitivity. Skeletal muscle was examined for lipid metabolism. The results suggest that EHP can significantly improve the glucose and lipid metabolism in DIO mice. *In vitro*, EHP inhibited the catalytic activity of recombinant human protein tyrosine phosphatase 1B (PTP1B) and reduced the protein and mRNA levels of PTP1B in the skeletal muscle. Moreover, expressions of genes related to fatty acid uptake and oxidation were changed by EHP in the skeletal muscle. These results suggest that EHP may improve insulin resistance and lipid metabolism in DIO mice. © 2014 The Authors. *Phytotherapy Research* published by John Wiley & Sons Ltd.

Keywords: *Hypericum perforatum L.*; PTP1B inhibitor; insulin resistance; dyslipidemia.

INTRODUCTION

Obesity and type 2 diabetes increase the numbers of death worldwide (Williams, 2008). Insulin resistance is a key factor in the etiology of type 2 diabetes and other obesity-related chronic diseases (Grundy, 2006; Ye, 2013). Lipid metabolic disorder plays an important role in insulin resistance (Novgorodtseva *et al.*, 2011; Takasu *et al.*, 2012). The intramyocellular lipid accumulation is associated with insulin resistance and recognized as a hallmark of type 2 diabetes in obese humans and animals (Haus *et al.*, 2011; Korach-André *et al.*, 2005; Kuhlmann *et al.*, 2005; Raz *et al.*, 2005). Treatment of insulin resistance is limited by the availability of effective and safe medicines (Ye, 2011).

Protein tyrosine phosphatase 1B (PTP1B), the negative regulator of insulin and leptin signaling pathways, has been considered as a promising molecular target in the treatment of insulin resistance and lipid metabolic

disorder (Basavarajappa *et al.*, 2012; Johnson *et al.*, 2002; Sun *et al.*, 2007). PTP1B inhibition leads to improvement in insulin signaling and fatty acid oxidation in muscles (Zabolotny *et al.*, 2004; Zhang, 2002). So, numerous efforts directly towards the discovery of specific PTP1B inhibitors have been made.

Natural product *Hypericum perforatum L.* has been used in folk medicine to improve mental performance. It contains several kinds of chemical compounds, such as flavonoids, proanthocyanidins, naphthodianthrones (including hypericin and pseudohypericin), and acylphloroglucinols (including hyperforin and adhyperforin) (Nahrstedt and Butterweck, 1997). Recently, evidence suggests that *H. perforatum L.* has multiple activities with potential pharmacological interest, including antibacterial, antitumoral, and antiangiogenic effects (Medina *et al.*, 2006). However, it is still unknown whether *H. perforatum L.* has an effect on metabolic syndrome. Here, we found that the extract from *H. perforatum L.* (EHP) inhibited PTP1B and improved insulin resistance and lipid metabolism.

MATERIALS AND METHODS

Plant material and extractions. The aerial parts of *H. perforatum L.* were collected in Huocheng County, Xinjiang, China, and identified by Prof. Fa Liu of Xinjiang Institute of Materia Medica. The voucher specimen (ID-S-2250) was deposited at the herbarium of Institute

* Correspondence to: Teng-fei Ji, State Key Laboratory of Bioactive Substance and Function of Natural Medicines, Institute of Materia Medica, Chinese Academy of Medical Sciences, Beijing 100050, China.; Fei Ye, Beijing Key Laboratory of New Drug Mechanisms and Pharmacological Evaluation Study, Institute of Materia Medica, Chinese Academy of Medical Sciences, Beijing 100050, China.
E-mail: yefei@imm.ac.cn (Fei Ye); jitf@imm.ac.cn (Teng-fei Ji)

This is an open access article under the terms of the Creative Commons Attribution-NonCommercial License, which permits use, distribution and reproduction in any medium, provided the original work is properly cited and is not used for commercial purposes.

of Materia Medica, Chinese Academy of Medical Sciences, China. The dried aerial parts of *H. perforatum L.* were extracted with 95% ethanol at room temperature. The solvent was removed under reduced pressure for isolation of the extract. To this extract, H₂O was added and the solution was filtered with a Diaion HP-20 column. The retained compounds were eluted from the column with H₂O-95% ethanol (1:0-0:1) to yield four fractions. The fraction 4 was named as EHP (the extraction rate was about 0.75% of dry weight of *H. perforatum L.*), and the chemical character was determined with thin-layer chromatography, ultraviolet (UV) and high-performance liquid chromatography (HPLC), HPLC-mass spectrometry (MS) fingerprint analysis, respectively.

Data analysis: In order to identify the chemical components in the extract, the fingerprints of EHP were analyzed using the on-line diode array detection-electrospray ionization (DAD-ESI)-MS techniques. It was found that the negative mode contained more ions than the positive mode; therefore, ESI in the negative mode was selected for the following analysis.

HPLC analysis: HPLC analysis was performed with an Agilent 1100 series system (Palo Alto, CA, USA). An Agilent Zorbax Eclipse XDB-C18 column (150 mm × 2.1 mm, i.d., 5 μm) at 35 °C eluted 30% 20 mM NH₄AC water solution (A) and 70% CH₃CN(B) in 30 min at a flow rate of 0.3 mL/min, which was monitored at 590 nm.

LC-MS analysis: The MS analysis was performed using an Agilent 1100 series LC/MSD Trap system, the conditions of HPLC as An Agilent Zorbax Eclipse XDB-C18 column (150 mm × 2.1 mm, i.d., 5 μm) maintained at 35 °C. The mobile phase was 30% 20 mM NH₄AC water solution (A) and 70% CH₃CN (B) in 30 min at a flow rate of 0.3 mL/min, monitored at 590 nm. The conditions of the ESI source were as follows: source voltage, 3500 V; drying gas (N₂) flow rate 9.00 L/min; drying gas temperature, 35 °C; pressure of nebulizer, 40.00 psi. Scan range of MS spectra was set between 100 U and 1000 U in negative mode.

Animals and treatments. Four-week-old, male C57BL/6J mice were obtained from the Animal Center of the Institute of Laboratory Animal Sciences, Chinese Academy of Medical Sciences. The animals were housed at 21–23 °C and at a humidity level of 40–60%. They were

exposed to a 12-h lighting cycle (06:00–18:00 light, 18:00–06:00 dark) and had free access to water and diets. After a 14-week feeding with the high-fat-diet (50% fat, 36% carbohydrate, and 14% protein in calorie), the DIO mice were randomly divided into four groups: untreated (Model), Rosi (positive control), EHP-L (low dose), and EHP-H (high dose). These groups were treated with water, rosiglitazone (15 mg/kg/day), EHP 50 mg/kg/day and 200 mg/kg/day by gavage (once a day) for 3 weeks. In addition, age-matched male C57BL/6J mice, fed with chow (12% fat, 62% carbohydrate, and 26% protein in calorie), were used as normal control (Con). All experimental procedures were approved by the Animal Care and Use Committee in our institute.

The oral glucose tolerance test (OGTT), the insulin tolerance test (ITT), and the hyperinsulinemic-euglycemic clamp test were performed as described previously (Ye *et al.*, 2008) with some modification. The PTP1B activity was determined according to the method reported (Ma *et al.*, 2011).

Materials. Commercial kits for the measurements of serum triglyceride (TG) and total cholesterol (TC) were obtained from BIOSINO Bio-Technology and Science INC (Beijing, China). Insulin was purchased from Novo Nordisk (Denmark); sodium pentobarbital, glucose, and other reagents were purchased from the Beijing Chemical Reagents Company (Beijing, China). The reagents para-NitroPhenyl Phosphate (pNPP) and para-nitrophenol (pNP) were produced by Sigma-Aldrich Trading Co., Ltd., USA. Anti-PTP1B antibody was obtained from Upstate (CA, USA), and anti-Actin antibody were purchased from Santa Cruz Biotechnology (CA, USA).

Biochemical assays. Blood glucose level was determined with a glucose analyzer (Biosen 5030, EKF Diagnostic, Germany). Protein concentration was determined with the Bio-Rad protein assay reagent (Bio-Rad, Hercules, CA, USA) with a microplate spectrophotometer (μQuant, BioTek Instruments, Inc, USA). The TG and TC levels were determined according to the instructions in the assay kit. Muscle triglyceride content was determined as glycerol residues after extraction and separation of the muscle samples according to the methods as reported (Ragheb *et al.*, 2009). Serum insulin

Table 1. Sequences of the primers used in the PCR measurements

Gene	Sense	Sequence (5' to 3')	Gen bank no./ref.
PTP1B	Forward	TTCTCCTACCTGGCTGTCATCG	NM 011201
	Reverse	CCCACCATCCGTCTCCTAACT	
ACCβ	Forward	CTGCTCCAGGCTAAGCGATT	NM 133904.1
	Reverse	AGCCGATTTGGAAGGTGATG	
CD36	Forward	TGTACCTGGGAGTTGGCGAG	NM 007643
	Reverse	CTGCTGTTCTTTGCCACGTC	
FATP1	Forward	AGCCATCTGGGAGGAGTTCA	NM 011977
	Reverse	AGAGGGTCTGCTGGTTGAT	
CPT-1	Forward	GTTCAACACTACACGCATCCC	NM 009948
	Reverse	GGTCACAAAGAAAGCAGCAC	
Actin	Forward	CCCATCTACGAGG GCTAT	NM 007393
	Reverse	TGGCC AGTAA TGTC AGG	

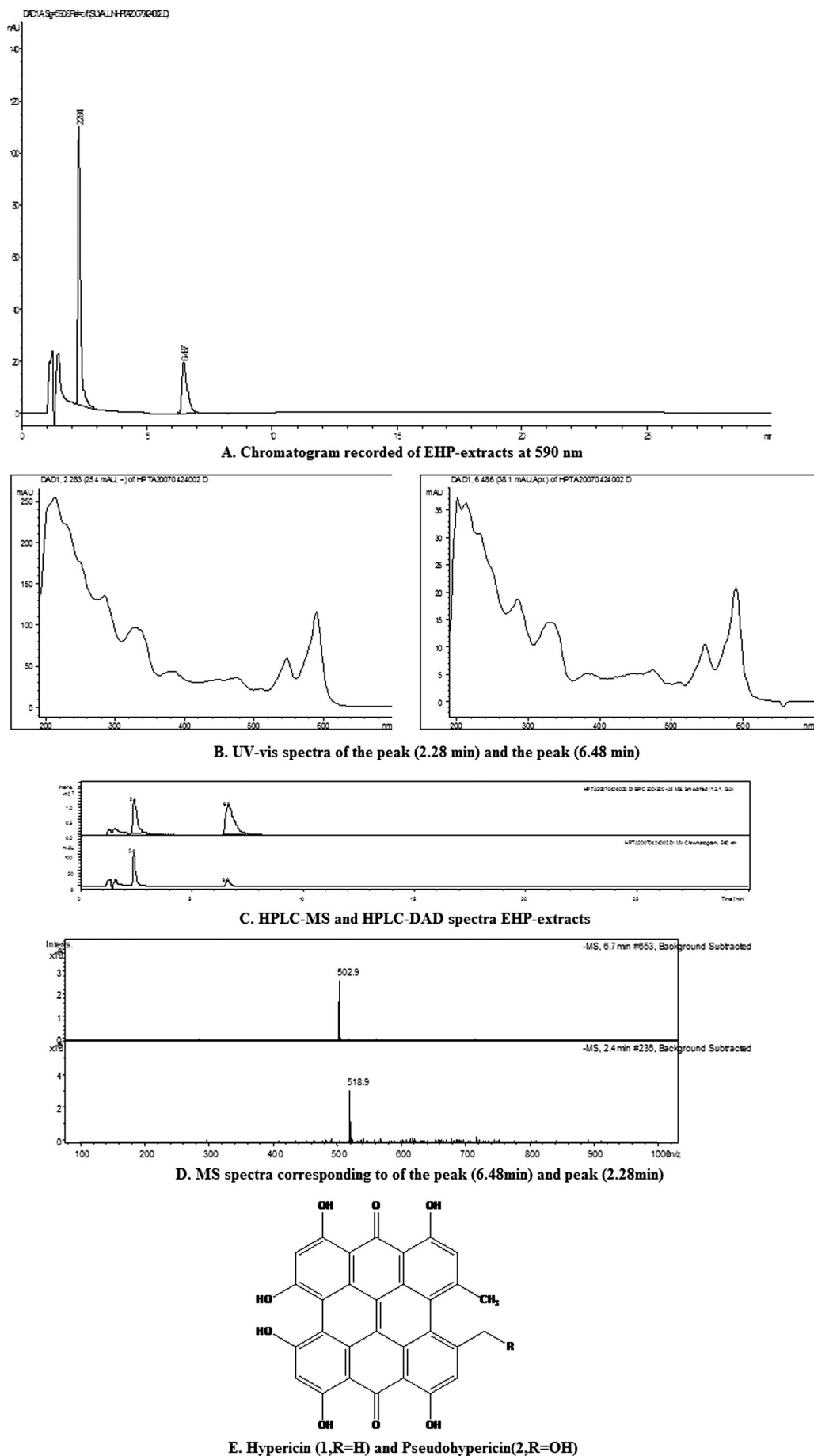


Figure 1. EHP-HPLC fingerprint analysis A, Chromatogram recorded of EHP-extracts at 590 nm; B, UV-vis spectra of peak (2.28 min) and peak (6.48 min); C, HPLC-MS and HPLC-DAD spectra EHP-extracts; D, MS spectra corresponding to the peak (2.28 min and 6.48 min); E, Hypericin (1, R = H) and Pseudohypericin (2, R = OH).

concentration was estimated with a radioimmunoassay kit obtained from the Northern Bioengineering Institute (Beijing, China) using a liquid scintillation and luminescence counter (1450 MicroBeta, PerkinElmer, USA).

The mRNA levels were analyzed by reverse transcription polymerase chain reaction (RT-PCR). Total RNA was isolated from skeletal muscle with Trizol reagent and reverse transcribed by a two-step method with the Super Script First-Strand Synthesis System. The samples were chosen randomly from each group, and the assay of every gene (Table 1) in each sample was replicated three times. The β -actin gene was

amplified as a loading control. The PCR products were separated by electrophoresis on a 1% agarose gel.

The protein expression was estimated by western blot analysis with the method reported (Ma *et al.*, 2011). Immunoblotting analysis was performed with enhanced chemiluminescence (ECL) reagent and detected by a gel analysis system (Fluorochem 5500, Alpha Innotech, USA).

Statistical analysis. Data were analyzed by SPSS version 11.0. All results are expressed as mean \pm SD (standard deviation). *P* values less than 0.05 were considered statistically significant.

Table 2. Insulin sensitivity related plasma parameters in mice

	FBG (mg/dL)	FINS (μ IU/L)	HOMA-IR (mg/dl \times μ IU/L)
Con	74.1 \pm 15.4	6.8 \pm 2.8	23.5 \pm 13.3
Model	105.7 \pm 14.4 ^{###}	54.2 \pm 34.7 ^{###}	284.5 \pm 151.7 ^{###}
Rosi	76.4 \pm 11.2 ^{***}	9.3 \pm 2.5 ^{**}	30.8 \pm 4.6 ^{***}
EHP-L	81.5 \pm 32.6 [*]	19.2 \pm 7.3 ^{**}	72.2 \pm 46.8 ^{**}
EHP-H	95.7 \pm 19.3	16.4 \pm 4.4 ^{**}	72.4 \pm 32.1 ^{***}

FBG, the level of fasting blood glucose; FINS, the level of fasting serum insulin. HOMA-IR index was calculated by the formula (HOMA-IR = FINS \times FBG/22.5). *n* = 9.

^{###}, *P* < 0.001 vs Con; *, **, ***, *P* < 0.05, 0.01, 0.001 vs Model.

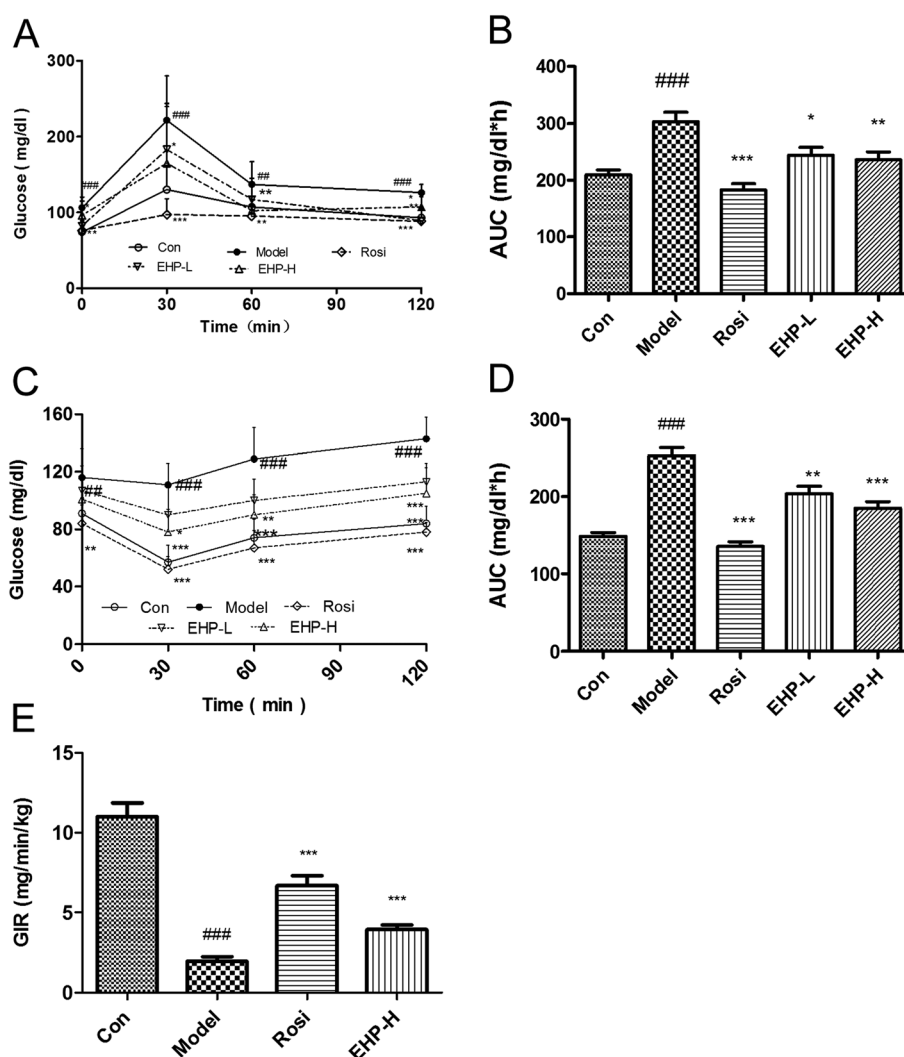


Figure 2. Effects of EHP on insulin resistance in mice A, Blood glucose levels in OGTT; B, Areas under the blood glucose-time curves in OGTT; C, Blood glucose levels in ITT; D, Areas under the blood glucose-time curves in ITT; E, GIR value in hyperinsulinemic-euglycemic clamp test. *n* = 9. #*P* < 0.05, ##*P* < 0.01, ###*P* < 0.001 vs Con; **P* < 0.05, ***P* < 0.01, ****P* < 0.001 vs Model.

RESULTS

EHP extraction and isolation procedures

In the chromatogram recorded of EHP extracts at 590 nm (Fig. 1A), two peaks were found, $R_t=2.28$ min and $R_t=6.48$ min; and 590 nm in their UV-vis spectra (Fig. 1B) was the characteristic signal of naphthodianthrone.

In the negative ESI-MS spectra of EHP-extracts (Fig. 1C, D) the quasi-molecular ion peaks of $R_t=2.28$ min and $R_t=6.48$ min appear m/z 518.9 and 502.9 as $[M-H]^-$ ions, we finally tentatively elucidated compounds to be hypericin (1, $R_t=6.48$ min) and pseudohypericin (2, $R_t=2.28$ min) (Fig. 1E) combined with UV-vis spectra. EHP extract was separated and identified by means of HPLC-MS analysis that it contained mainly hypericin analogues.

Effects of EHP on insulin resistance

After feeding with the high-fat-diet for 14 weeks, DIO mice developed significant insulin resistance. Fasting insulin and the homeostasis model assessment of insulin resistance (HOMA-IR) index were increased by 12.11 and 7.97 folds compared with those in the chow group. After 1-week treatment, the levels of serum insulin and HOMA-IR were markedly decreased by 64.6% and 74.6% in EHP-L group, and by 69.7% and 74.6% in EHP-H group. Similar results were observed in Rosi group (Table 2). These data suggest that EHP is able to improve insulin sensitivity in DIO mice.

After EHP treatment for 1 week, OGTT was performed. The blood glucose and the area under the curve (AUC) in Model group were significantly higher than those in the chow control group. Compared with those in Model group, the levels of blood glucose at 30, 60, and 120 min were decreased by 28.6% in EHP-L group and

by 36.0% in EHP-H group; and the AUC values were also decreased by 19.6% and 22.4% in EHP-L and EHP-H groups (Fig. 2A, B). Similar results were obtained in Rosi group. These data suggest that EHP is able to improve glucose metabolism in DIO mice.

After EHP treatment for 1 week, ITT was performed. The blood glucose level was decreased by 36.9% in chow group and by 4.3% in Model group at 30 min, compared with their own baseline. The AUC value in Model group was much higher than that in chow group. As expected, the mice treated with EHP exhibited an enhanced ability of glucose clearance in ITT. There was a greater decline in blood glucose levels by 16.6% and 30.0% in EHP-L and EHP-H groups. The reduction was associated with 19.7% and 29.9% reduction in AUC compared with those in Model group (Fig. 2C, D). The effect of EHP was similar to that of rosiglitazone in ITT. The data suggest that EHP is able to improve insulin tolerance in DIO mice and the activity is comparable to rosiglitazone.

In order to confirm insulin sensitizing effect of EHP, the hyperinsulinemic-euglycemic clamp test was performed in mice after EHP treatment for 2 weeks. The value of the glucose infusion rate (GIR) was 5.5-fold lower in Model group than that in chow group. After rosiglitazone

Table 3. Effects of EHP on lipid profiles in high-fat-fed mice

	Serum TC (mg/dL)	Serum TG (mg/dL)	Muscle TG (mg/g pro)
Con	83 ± 7	114 ± 38	3.0 ± 0.6
Model	216 ± 28 ^{###}	84 ± 14 [#]	4.5 ± 0.9 ^{##}
Rosi	199 ± 18	47 ± 11 ^{***}	4.4 ± 1.3
EHP-L	181 ± 26 [*]	73 ± 16	4.1 ± 1.2
EHP-H	168 ± 30 ^{**}	65 ± 19 [*]	3.4 ± 0.8 [*]

$n = 9$. #, ##, ###, $P < 0.05$, 0.01, 0.001 vs Con; *, **, ***, $P < 0.05$, 0.01, 0.001 vs Model.

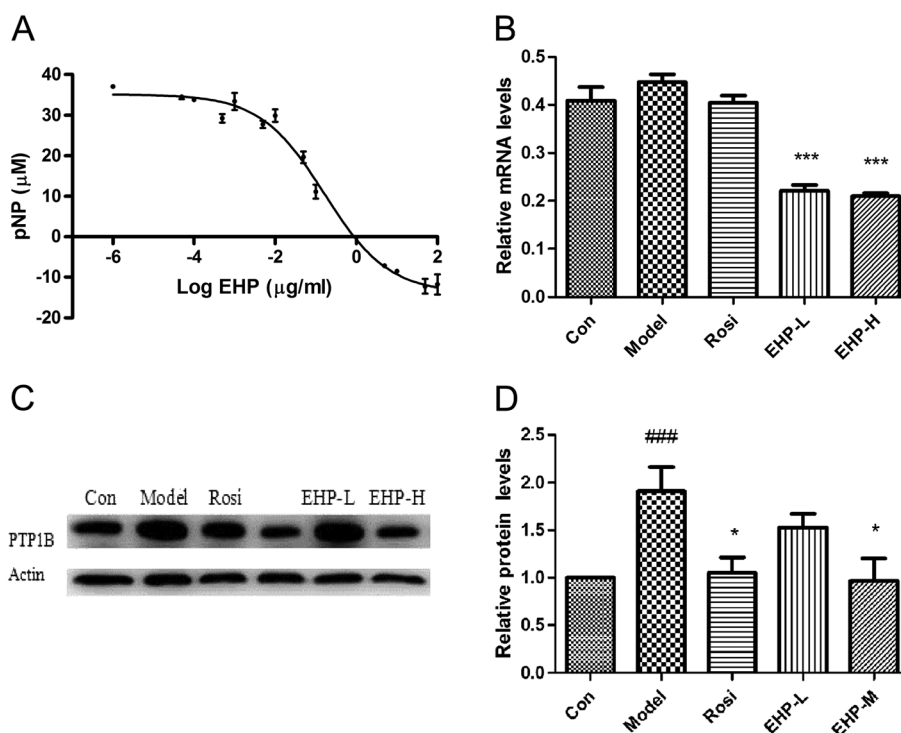


Figure 3. Effects of EHP on target PTP1B A, Inhibition on recombinant hPTP1B protein activity, $n = 3$; B, The mRNA levels of PTP1B in skeletal muscle, $n = 5$; C, The expression of PTP1B in skeletal muscle. # $P < 0.05$, ### $P < 0.001$ vs Con; * $P < 0.05$, *** $P < 0.001$ vs Model.

and EHP treatments, the GIR values were increased by 240% and 101% in Rosi and EHP-H groups, respectively, compared with that in Model group (Fig. 2E).

Inhibition of PTP1B by EHP

In order to understand the mechanism by which EHP improves insulin sensitivity, we tested EHP for inhibition of PTP1B *in vitro*. EHP exhibited a strong inhibitory effect on the catalytic activity of recombinant hPTP1B protein with an EC₅₀ of 1.08 µg/mL (Fig. 3A).

After treatment with EHP for 3 weeks, the mRNA levels of PTP1B were decreased by 32.8% and 50.7% in a dose dependent manner in the skeletal muscle of the EHP-L and EHP-H groups (Fig. 3B). Meanwhile, the protein levels of PTP1B were markedly up-regulated in the skeletal muscle of DIO mice, and the increase was reversed by 21.8% and 48.8% in EHP-L and EHP-H groups (Fig. 3C).

Effects of EHP on lipid metabolic profiles

DIO mice developed hypercholesterolemia, but not hypertriglyceridemia. Compared with the levels in DIO mice, the serum TC was significantly decreased by 16.2% and 22.2%, and the levels of serum TG were decreased by 13.1% and 22.6% in the EHP-L and EHP-H groups in a dose-dependent manner (Table 3).

The intramyocellular lipid accumulation in skeletal muscle has been associated with insulin resistance and dyslipidemia. The results showed that triglyceride content in the skeletal muscles was significantly increased in DIO mice, and the change was reversed by EHP treatment. Compared with those in DIO mice, the triglyceride contents in the skeletal were decreased by 8.9% and 25.3% in EHP-L and EHP-H groups in a dose-dependent manner (Table 3).

Effects of EHP on the lipid metabolic pathways in the skeletal muscle

In order to understand the mechanisms of EHP action on dyslipidemia, gene expression was examined for those involved in lipid metabolism. As a major transporter of fatty acid, FATP1, was significantly increased in the skeletal muscle of DIO mice. Also, EHP decreased the gene expression of FATP1 in a dose-dependent manner. However, there were no significant changes in mRNA levels of CD36 from EHP treatment (Fig. 4).

As an important regulator of fatty acid oxidation, CPT-1 was mildly increased in the skeletal muscle of DIO mice. EHP increased CPT-1 expression at the high dosage. The mRNA level of ACCβ was higher in Model group than that in chow group, and the change was reversed by EHP treatment (Fig. 4).

DISCUSSION

Insulin resistance, characterized by reduced responsiveness to circulating insulin, is a common feature in type 2 diabetes (Ye, 2013; Choudhary *et al.*, 2012). DIO mice are

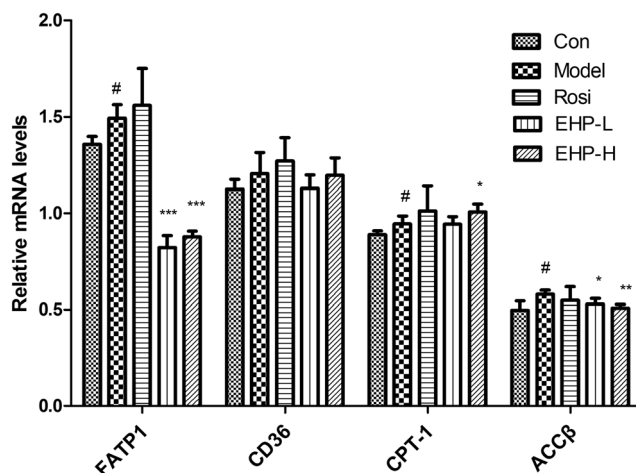


Figure 4. Effects of EHP on the factors involved fatty acid metabolism in skeletal muscle. Each sample was from 3 independent experiments of 9 mice. # $P < 0.05$ vs Con; * $P < 0.05$, ** $P < 0.01$, *** $P < 0.001$ vs Model.

characterized with obesity and insulin resistance and area valuable tool in the study of insulin sensitizer (Almind and Kahn, 2004; Biddinger and Ludwig, 2005). Consistently, our results showed the mice challenged with high-fat-diet developed serious insulin resistance and dyslipidemia.

As the largest organ in the body, the skeletal muscle plays a very important role in the glucose and lipid metabolism (Pedersen and Febbraio, 2012). Many proteins produced by the skeletal muscle may be involved in the association between sedentary behavior and chronic diseases such as cardiovascular diseases, type 2 diabetes. Therefore, our study of EHP was conducted in the skeletal muscle.

Defects in the insulin signaling cascade play a key role in the pathogenesis of insulin resistance (Choi and Kim, 2010; Ye, 2013). PTP1B is a negative regulator of both insulin and leptin signaling through antagonizing the activities of insulin receptor and Janus kinase 2 (JAK2) (Koren and Fantus, 2007). Whole-body Ptp1b^{-/-} mice show enhanced insulin sensitivity and increased phosphorylation of tyrosine residues on insulin receptor (Klaman *et al.*, 2000). PTP1B inhibitor can augment insulin sensitivity through enhancing insulin receptor and leptin receptor activities (Picardi *et al.*, 2008). Here, both the catalytic activity and gene expression of PTP1B were decreased by EHP treatment, suggesting that EHP is an inhibitor of PTP1B. EHP led to improvement of hyperinsulinemia, hyperglycemia, insulin tolerance, and GIR in the hyperinsulinemic–euglycemic clamp test.

PTP1B is a molecular target for lipid disorder in addition to insulin sensitization (Picardi *et al.*, 2008). EHP can decrease the serum triglyceride, cholesterol, and ectopic lipid accumulation in skeletal muscle. The putative mechanism is increasing fatty acid oxidation in skeletal muscle of DIO mice.

Insulin resistance in skeletal muscle is associated with intramuscular lipid accumulation, which is a result of insulin signaling inhibition by lipids (Holland *et al.*, 2007). FATP1 that mediates fatty acid uptake into cells is implicated in the development of insulin resistance. FATP1 deletion in KO mice protected mice from fat-induced insulin resistance and intramuscular accumulation of fatty acyl-CoA (Kim *et al.*, 2004). FATP1 inactivation led to reduction in skeletal muscle lipid accumulation and improvement in insulin sensitivity (Wu *et al.*, 2006). In this study, the mRNA levels of FATP1 in DIO mice were

increased by HFD and reduced by EHP. FATP1 reduction may explain the decreased TG content in skeletal muscle of EHP groups. ACC β catalyzes malonyl CoA formation and high expression of ACC β increases malonyl CoA level, which lead to inhibition of CPT-1 activity. CPT-1 inhibition results in suppression of the fatty acid β -oxidation and increase in intracellular lipid accumulation (Cheng *et al.*, 2002). Here, EHP significantly increased mRNA levels of genes related to fatty acid oxidation, suggesting that EHP regulates fatty acid oxidation. However, EHP did not markedly decrease the liver TG content (date not shown). These results suggested that the skeletal muscles might be the major target tissue of EHP.

In conclusion, the present results demonstrated that EHP, an extraction from *H. perforatum L.*, serves as a

new PTP1B inhibitor. It improves insulin resistance and dyslipidemia in DIO C57BL/6J mice. EHP is a potential drug candidate in the treatment of metabolic syndrome.

Acknowledgements

This work was supported by the National Major Special Project on New Drug Innovation of China (no. 2012ZX09103-101-063; 2012ZX09301002-004). We thank Prof. Fa Liu of Xinjiang Institute of Materia Medica (China) for the plant identification and Servier Company (France) for the kind contribution of PTP1B plasmid.

Conflict of interest

The authors declare no conflict of interest.

REFERENCES

- Almind K, Kahn CR. 2004. Genetic determinants of energy expenditure and insulin resistance in diet-induced obesity in mice. *Diabetes* **53**: 3274–3285.
- Basavarajappa DK, Gupta VK, Rajala RV. 2012. Protein Tyrosine Phosphatase 1B: A Novel Molecular Target for Retinal Degenerative Diseases. *Adv Exp Med Biol* **723**: 829–834.
- Biddinger SB, Ludwig DS. 2005. The insulin-like growth factor axis: a potential link between glycemic index and cancer. *Am J Clin Nutr* **82**: 277–278.
- Cheng A, Uetani N, Simoncic PD *et al.* 2002. Attenuation of leptin action and regulation of obesity by protein tyrosine phosphatase 1B. *Dev Cell* **2**: 497–503.
- Choi K, Kim YB. 2010. Molecular mechanism of insulin resistance in obesity and type 2 diabetes. *Korean J Intern Med* **25**: 119–129.
- Choudhary N, Kalra S, Unnikrishnan AG *et al.* 2012. Preventive pharmacotherapy in type 2 diabetes mellitus. *Indian J Endocrinol Metab* **16**: 33–43.
- Grundy SM. 2006. Drug therapy of the metabolic syndrome: minimizing the emerging crisis in polypharmacy. *Nat Rev Drug Discov* **5**: 295–309.
- Haus JM, Solomon TP, Lu L *et al.* 2011. Intramyocellular lipid content and insulin sensitivity are increased following short-term low-glycemic index diet and exercise intervention. *Am J Physiol Endocrinol Metab* **301**: E511–E516.
- Holland WL, Knotts TA, Chavez JA *et al.* 2007. Lipid mediators of insulin resistance. *Nutr Rev* **65**(6 Pt 2): S39–S46.
- Johnson TO, Ermoloeff J, Jirousek MR. 2002. Protein tyrosine phosphatase 1B inhibitors for diabetes. *Nat Rev Drug Discov* **1**: 696–709.
- Kim JK, Gimeno RE, Higashimori T *et al.* 2004. Inactivation of fatty acid transport protein 1 prevents fat-induced insulin resistance in skeletal muscle. *J Clin Invest* **113**: 756–763.
- Klaman LD, Boss O, Peroni OD *et al.* 2000. Increased energy expenditure, decreased adiposity, and tissue-specific insulin sensitivity in protein-tyrosine phosphatase 1B-deficient mice. *Mol Cell Biol* **15**: 5479–5489.
- Korach-André M, Gounarides J, Deacon R *et al.* 2005. Age and muscle-type modulated role of intramyocellular lipids in the progression of insulin resistance in nondiabetic Zucker rats. *Metabolism* **54**: 522–528.
- Koren S, Fantus IG. 2007. Inhibition of the protein tyrosine phosphatase PTP1B: potential therapy for obesity, insulin resistance and type-2 diabetes mellitus. *Best Pract Res Clin Endocrinol Metab* **21**: 621–640.
- Kuhlmann J, Neumann-Haefelin C, Belz U *et al.* 2005. Correlation between insulin resistance and intramyocellular lipid levels in rats. *Magn Reson Med* **53**: 1275–1282.
- Ma YM, Tao RY, Liu Q *et al.* 2011. PTP1B inhibitor improves both insulin resistance and lipid abnormalities in vivo and in vitro. *Mol Cell Biochem* **357**: 65–72.
- Medina MA, Martínez-Poveda B, Amores-Sánchez MI *et al.* 2006. Hyperforin: more than an antidepressant bioactive compound? *Life Sci* **79**: 105–111.
- Nahrstedt A, Butterweck V. 1997. Biologically active and other chemical constituents of the herb of *Hypericum perforatum L.* *Pharmacopsychiatry* **2**: 129–134.
- Novgorodtseva TP, Karaman YK, Zhukova NV *et al.* 2011. Composition of fatty acids in plasma and erythrocytes and eicosanoids level in patients with metabolic syndrome. *Lipids Health Dis* **10**: 82.
- Pedersen BK, Febbraio MA. 2012. Muscles, exercise and obesity: skeletal muscle as a secretory organ. *Nat Rev Endocrinol* **8**: 457–465.
- Picardi PK, Calegari VC, Prada PO *et al.* 2008. Reduction of hypothalamic protein tyrosine phosphatase improves insulin and leptin resistance in diet-induced obese Rats. *Endocrinology* **149**: 3870–3880.
- Ragheb R, Shanab GM, Medhat AM *et al.* 2009. Free fatty acid-induced muscle insulin resistance and glucose uptake dysfunction: Evidence for PKC activation and oxidative stress-activated signaling pathways. *Biochem Biophys Res Commun* **389**: 211–216.
- Raz I, Eldor R, Cernea S, Shafir E. 2005. Diabetes: insulin resistance and derangements in lipid metabolism. Cure through intervention in fat transport and storage. *Diabetes Metab Res Rev* **21**: 3–14.
- Sun T, Wang Q, Yu Z *et al.* 2007. Hyrtiosal, a PTP1B inhibitor from the marine sponge *Hyrtios erectus*, shows extensive cellular effects on PI3K/AKT activation, glucose transport, and TGF β /Smad2 signaling. *ChemBioChem* **8**: 187–193.
- Takasu S, Mutoh M, Takahashi M *et al.* 2012. Lipoprotein lipase as a candidate target for cancer prevention/therapy. *Biochem Res Int* **2012**: 398697.
- Williams KJ. 2008. Molecular processes that handle-and mishandle-dietary Lipids. *J Clin Invest* **118**: 3247–3259.
- Wu Q, Ortegon AM, Tsang B *et al.* 2006. FATP1 is an insulin-sensitive fatty acid transporter involved in diet-induced obesity. *Mol Cell Biol* **26**: 3455–3467.
- Ye J. 2011. Challenges in drug discovery for thiazolidinedione substitute. *Acta Pharma Sinica B* **1**: 137–142.
- Ye J. 2013. Mechanisms of insulin resistance in obesity. *Front Med* **7**: 14–24.
- Ye F, Tao R, Cong W *et al.* 2008. Utilization of fluorescence tracer in hyperinsulinemic-euglycemic clamp test in mice. *J Biochem Biophys Methods* **70**: 978–984.
- Zabolotny JM, Haj FG, Kim YB *et al.* 2004. Transgenic overexpression of protein-tyrosine phosphatase 1B in muscle causes insulin resistance, but overexpression with leukocyte antigen-related phosphatase does not additively impair insulin action. *J Biol Chem* **279**: 24844–24851.
- Zhang YZ. 2002. Protein tyrosine phosphatases: structure and function, substrate specificity, and inhibitor development. *Annu Rev Pharmacol Toxicol* **42**: 209–234.